Whole genome sequencing identifies candidate genes for familial essential tremor and reveals biological pathways implicated in essential tremor aetiology

Lorraine N. Clark,[a,b,1]*** Yizhe Gao,[c,d,e] Gao T. Wang,[c,d,e] Nora Hernandez,[f] Allison Ashley-Koch,[g] Joseph Jankovic,[h] Ruth Ottman,[c,d,i,j] Suzanne M. Leal,[b,c,d,e] Sandra M. Barral Rodriguez,[b,c,d,1]** and Elan D. Louis [f,1]*

[a]Department of Pathology and Cell Biology, Vagelos College of Physicians and Surgeons, Columbia University Irving Medical Center, New York, NY, USA

[b]The Taub Institute for Research on Alzheimer's Disease and The Aging Brain, Columbia University Irving Medical Center, New York, NY, USA

[c]The G.H. Sergievsky Center, Vagelos College of Physicians and Surgeons, Columbia University Irving Medical Center, New York, NY, USA

[d]Department of Neurology, Vagelos College of Physicians and Surgeons, Columbia University Irving Medical Center, New York, NY, USA

[e]The Center for Statistical Genetics, Columbia University Irving Medical Center, New York, NY, USA

[f]Department of Neurology, University of Texas Southwestern Medical Center, Dallas TX, USA

[g]Duke Molecular Physiology Institute, Duke University Medical Center, Durham, NC, USA

[h]Parkinson's Disease Center and Movement Disorders Clinic, Department of Neurology, Baylor College of Medicine, Houston TX, USA

[i]Department of Epidemiology, Mailman School of Public Health, Columbia University Irving Medical Center, New York, NY, USA

[j]Division of Translational Epidemiology, New York State Psychiatric Institute, New York, NY, USA

Summary

Background Essential tremor (ET), one of the most common neurological disorders, has a phenotypically heterogeneous presentation characterized by bilateral kinetic tremor of the arms and, in some patients, tremor involving other body regions (e.g., head, voice). Genetic studies suggest that ET is genetically heterogeneous.

Methods We analyzed whole genome sequence data (WGS) generated on 104 multi-generational white families with European ancestry affected by ET. Genome-wide parametric linkage and association scans were analyzed using adjusted logistic regression models through the application of the Pseudomarker software. To investigate the additional contribution of rare variants in familial ET, we also performed an aggregate variant non-parametric linkage (NPL) analysis using the collapsed haplotype method implemented in CHP-NPL software.

Findings Parametric linkage analysis of common variants identified several loci with significant evidence of linkage (HLOD ≥3.6). Among the gene regions within the strongest ET linkage peaks were *BTC* (4q13.3, HLOD=4.53), *N6AMT1* (21q21.3, HLOD=4.31), *PCDH9* (13q21.32, HLOD=4.21), *EYA1* (8q13.3, HLOD=4.04), *RBFOX1* (16p13.3, HLOD=4.02), *MAPT* (17q21.31, HLOD=3.99) and *SCARB2* (4q21.1, HLOD=3.65). CHP-NPL analysis identified fifteen additional genes with evidence of significant linkage (LOD ≥3.8). These genes include *TUBB2A, VPS33B, STEAP1B, SPINK5, ZRANB1, TBC1D3C, PDPR, NPY4R, ETS2, ZNF736, SPATA21, ARL17A, PZP, BLK* and *CCDC94*. In one ET family contributing to the linkage peak on chromosome 16p13.3, we identified a likely pathogenic heterozygous canonical splice acceptor variant in exon 2 of *RBFOX1* (ENST00000547372; c.4-2A>G), that co-segregated with the ET phenotype in the family.

*Corresponding author at: Linda and Mitch Hart Distinguished Chair in Neurology, Chair, Department of Neurology, University of Texas Southwestern Medical Center, Dallas, TX, USA.

**Corresponding author at: Neurogenetics, Department of Neurology, Columbia University Irving Medical Center, New York, NY, USA.

***Corresponding author at: Pathology and Cell Biology, Department of Pathology and Cell Biology, Taub Institute, Columbia University Irving Medical Center, New York, NY, USA.

E-mail addresses: lc654@cumc.columbia.edu (L.N. Clark), smb2174@cumc.columbia.edu (S.M.B. Rodriguez), Elan.Louis@UTSouthwestern.edu (E.D. Louis).

[1] Authors contributed equally to this work.

Interpretation Linkage and association analyses of WGS identified several novel ET candidate genes, which are implicated in four major pathways that include 1) the epidermal growth factor receptor-phosphatidylinositol-4,5-bisphosphate 3-kinase catalytic subunit alpha-AKT serine/threonine kinase 1 (EGFR-PI3K-AKT) and Mitogen-activated protein Kinase 1 (ERK) pathways, 2) Reactive oxygen species (ROS) and DNA repair, 3) gamma-aminobutyric acid-ergic (GABAergic) system and 4) RNA binding and regulation of RNA processes. Our study provides evidence for a possible overlap in the genetic architecture of ET, neurological disease, cancer and aging. The genes and pathways identified can be prioritized in future genetic and functional studies.

Keywords: Essential tremor; Whole genome sequencing; Genome-wide linkage analysis; Multi-generation ET families

Research in Context

Evidence before this study

We searched PubMed for articles on Essential Tremor (ET) with no language restrictions up to September 2021, using the terms "Essential Tremor AND genetics" and Essential Tremor AND Linkage analysis". A number of previously published studies had conducted parametric and nonparametric linkage in multiplex ET families. However, no studies were found that had performed a joint linkage and linkage disequilibrium analysis using the software Pseudomarker, and an age dependent penetrance model, nor collapsed haplotype pattern (CHP) non-parametric linkage (CHP-NPL) analysis in ET families.

Added value of this study

To the best of our knowledge this is the first time a linkage scan has incorporated WGS, Pseudomarker (linkage and association) and a model-based analysis using an age dependence penetrance model, and aggregate variant non-parametric linkage (CHP-NPL) analysis in ET families. This study also includes, by far, the largest sample size to date with 104 multiplex ET families and 767 individuals. One of the hallmark features of the study was the meticulous approach to phenotyping, with all participants evaluated in person. Our study identifies several novel gene regions using Pseudomarker with suggestive linkage and association to ET (HLOD≥3.6). These regions contain functionally relevant candidate ET genes, which are implicated in four major pathways that include: 1) the EGFR-PI3K-AKT (*BTC, RBFOX1*) and ERK pathways (*COL9A2, DIAPH3* and *SOX8*), 2) ROS and DNA repair (*SCARB2, N6AMT1, EYA1* and *MAPT*), 3) GABAergic system (*PCDH9* and *NRXN3*) and 4) RNA binding and regulation of RNA processes (*STAU2* and *RBFOX1*). CHP-NPL identified significant linkage (LOD≥3.8) with 15 additional genes. These genes include *TUBB2A, VPS33B, STEAP1B, SPINK5, ZRANB1, TBC1D3C,*

PDPR, NPY4R, ETS2, ZNF736, SPATA21, ARL17A, PZP, BLK and *CCDC94*. Although none of the genes have previously been associated with ET, some of the genes cluster in the same pathways identified in the Pseudomarker analysis (e.g. EGFR-PI3K-AKT and ERK or DNA repair).

The identification of a likely pathogenic heterozygous canonical splice acceptor variant in exon 2 of *RBFOX1* (ENST00000547372; c.4-2A>G), that co-segregates with the ET phenotype in one family, nominates *RBFOX1* as an ET gene. *RBFOX1* binds to the C-terminus of ataxin 2 (SCA2) and among its related pathways are AKT signalling.

Implications of all the available evidence

Our study raises the possibility of shared genetic pathways in ET, neurological disease, cancer and ageing. The possible involvement of EGFR-PI3K-AKT signalling and ERK pathways in ET paves the way for functional studies and development of therapeutic strategies targeting these pathways. *LINGO-1,* which is upstream of the EGFR-PI3K-AKT signalling pathway, may represent a suitable therapeutic target. The human anti-LINGO-1 antibody Li81 (opicinumab), blocks LINGO-1 function and is currently being investigated in a Phase 2 clinical trial as a potential treatment for individuals with relapsing forms of Multiple Sclerosis (ClinicalTrials.gov, NCT03222973). Given the genetically heterogeneous nature of ET, further genetic studies in large patient populations and stratification based on genetic variation will be needed for therapeutic development.

Introduction

Essential tremor (ET) is a chronic, progressive neurologic disease.[1] Its hallmark feature is a 4-12 Hz kinetic tremor (i.e., a tremor that occurs during voluntary movements such as writing or eating) that involves the hands and arms. Tremor may also eventually spread to involve the head, voice and jaw and other body regions.[2]

Among the most prevalent adult-onset movement disorders, ET may occur at any age and paediatric cases have been reported,[3] but the majority of cases have adult age at onset. Meta-analysis of data from 42 population-based prevalence studies in 23 countries estimated that the pooled prevalence of ET across all ages was 1.33%, and prevalence increases with age to as much as 8.0% in persons 65 years and older.[4,5] Both genetic and environmental (toxic) factors are likely contributors to ET disease etiology.[6]

Clinical studies suggest the presence of substantial phenotypic heterogeneity in ET.[7] In addition to a spectrum of different types of tremor (kinetic, intention, postural, rest), other motor features can include gait ataxia and eye movement abnormalities and the presence of dystonia.[7] Non-motor features are also common in ET patients and may fall into a number of domains, including cognitive, neuropsychiatric (anxiety and depression), sleep-related and sensory (olfactory deficits in some studies, and hearing loss).[7] Numerous studies, from clinical to neuroimaging to pathological, provide evidence that the cerebellum is a brain region that is of prime importance in disease pathophysiology.[8−10]

Despite evidence of a genetic contribution to ET reported from twin studies[11,12] as well as family studies,[13,14] there has been a relative lack of progress in understanding the genetic aetiology of ET. This may be attributed to a number of factors, including the presence of substantial phenotypic and genotypic heterogeneity. Previous linkage studies, conducted assuming an autosomal dominant mode of inheritance with reduced penetrance in multiplex ET families, have failed to identify major susceptibility genes[15−21] and recent whole exome sequencing (WES) studies in ET families suggest the aetiology is due to private variants of strong effect in some families.[22−27] Some of the genes identified from WES with private variants in single families include FUS RNA binding protein (FUS), HtrA serine peptidase 2 (HTRA2), Teneurin transmembrane protein 4 (TENM4), Sortilin 1 (SORT1), Nitric oxide synthase 3 (NOS3), Potassium voltage-gated channel modifier subfamily S member 2 (KCNS2), Hyaluronan and proteoglycan link protein 4 (HAPLN4), Ubiquitin specific peptidase 46 (USP46), Calcium voltage-gated channel subunit alpha 1G (CACNA1G), and Slit guidance ligand 3 (SLIT3).[6,22−27]

Similarly, there has been a lack of replication of associations from genome-wide association studies (GWAS).[28−30]

The current study had two major goals: i) to apply a meticulous phenotyping approach to a large dataset of multiplex ET families (n=104) enrolled in the Family Study of Essential Tremor (FASET) and ii) to identify ET loci using parametric and non-parametric linkage analyses of WGS data.

Methods

Ethics

Study subjects and relatives were enrolled in a family study of ET at Columbia University NY and Yale University CT, USA, which was the then-home institution of one of the senior authors (E.D.L.). The study was approved by the Institutional Review Board at Columbia University (IRB-AAAQ3307) and Yale University (IRB-1412015096) and written informed consent was obtained from all participants.

Study subjects and clinical evaluation

One of the hallmark features of the study was the meticulous approach to phenotyping, with all 451 participants who were seen in person undergoing an extensive video-taped neurological examination that was reviewed (and could be repeatedly re-reviewed) by a senior movement disorders neurologist with special expertise in tremor (E.D.L.) using reliable and validated rating scales and diagnostic criteria. Details of the study, criteria for enrollment, and diagnosis of ET have been described previously.[25,31] There were 451 individuals with WGS data. All 451 individuals were evaluated in person and those affected with ET received a diagnosis of definite, probable, or possible ET. Diagnoses were based on the stringent criteria of the Washington Heights Inwood Genetic Study of ET (WHIGET), originally designed for population-based and family-based genetic studies.[32] All ET diagnoses were assigned by a senior movement disorders neurologist with a special expertise in tremor (E.D.L.) based on review of the history and a detailed videotaped neurological examination that included detailed assessments of action tremor, Parkinsonism and dystonia.[32,33] All these ET diagnoses (possible, probable and definite) required, at a minimum, moderate or greater amplitude kinetic tremor on at least three tasks (e.g., writing, drinking, pouring) or moderate or greater amplitude tremor in at least one task in the setting of head tremor and the absence of other aetiologies. As such, the criteria for all three categories of ET (i.e., possible, probable and definite) are even more stringent than those for definite ET that were outlined in the original Consensus Statement on Tremor of the Movement Disorders Society (published in 1998)[34] and the revised Consensus Criteria (published in 2018).[35] The clinical characteristics of study participants are summarized in Table 1. All pedigrees for the 104 ET Families included in the study are provided as Supplementary data (Supplementary Figure 1). To limit population stratification in genetic analyses, we restricted analysis to white participants. Ancestry information collected for participants was European.

There were 316 additional pedigree members with unknown affected status included in the pedigree file without WGS data. Family members with unknown

Families, n	104
Families with Ashkenazi Jewish ancestry, n (%)	11 (11.1%)
Subjects, n	451
Females, n (%)	254 (56.3)
Affected (Diagnosis of definite, probable or possible ET (n=330) and/or a diagnosis of Parkinson's disease, dystonia or mild tremor (n=20)	350 (77.6)
Average number (SD) of affected ET individuals per family[a]	5.7 (2.0)
Unaffected	101 (22.4)
Average number (SD) of unaffected individuals per family[a]	1.8 (1.6)
Age at Onset of affecteds[b], mean (SD)	31.2 (19.9)
Age (affecteds and unaffecteds), mean (SD)	60.2 (17.1)
Diagnosis of Definite, Probable or Possible ET (%) among 350 affecteds	330 (94.3%)
Diagnosis of Definite ET (%)	53 (16.1)
Diagnosis of Probable ET (%)	160 (48.5)
Diagnosis of Possible ET (%)	117 (35.4)
Diagnoses other than ET among 350 affecteds	20 (5.7%)
Diagnosis of Parkinson's disease (%)	2 (10.0)
Diagnosis of dystonia (%)	11 (55.0)
"Mild tremor" (%)[c]	7 (35.0)

***Table 1*: The demographic and clinical characteristics of study participants included in the parametric and nonparametric linkage analysis.**

[a] Includes affected or unaffected status for 451 enrolled subjects.
[b] Age of onset unavailable for n=47 affecteds.
[c] "Mild tremor": Has several kinetic tremor severity ratings of "1.5" or "2", and is likely developing ET, but does not yet meet criteria for possible ET.

affected status represent "dummy" variables (with unknown phenotypes and unknown parents) that were included to be able to reconstruct the pedigree structure.

Whole genome sequencing (WGS)

Genomic DNA was isolated from peripheral blood cells using standard methods. WGS was performed on the genomic DNA of individuals including affected (definite, probable, or possible ET diagnosis), and unaffected individuals from each of 104 families (n=451 individuals). Libraries were prepared using the TruSeq DNA PCR-free kit (Illumina San Diego CA USA). Paired-end sequencing (2 × 150 bp) was performed at >30x coverage per sample. Resulting libraries were sequenced on Illumina HiSeq TENx (Illuminia San Diego CA) at the New York Genome Center, NY. Sequence alignment to the UCSC hg19 reference genome was performed using the Burrows-Wheeler Aligner algorithm implemented in BWA,[36] duplicate reads were removed using Picard, and variant calling was performed using the Genome Analysis Toolkit (GATK4; Broad Institute Cambridge MA USA).[37] Local realignment and quality recalibration were performed via GATK4. Quality control checks for

samples were performed according to GATK4 best practices.

Quality control procedures

Pseudomarker. SNPs with a minor allele frequency (MAF) of $\geq 1\%$ as defined by the 1000 Genomes Project Phase 3, and a call rate of $\geq 90\%$ were retained for use in the analysis. The following criteria were used to filter and remove SNPs from the WGS dataset for the Pseudomarker analysis: 1) SNPs with MAF $<1\%$, 2) SNPs with MAF$\geq 1\%$ with call rate $<90\%$ or that were not in Hardy-Weinberg equilibrium.

CHP NPL analysis. All SNPs with a call rate of $\geq 90\%$ and that were in Hardy-Weinberg equilibrium were retained for use in the haplotype-level analysis through the CHP-NPL method.

Participants whose reported sex differed from the sex assignment determined by analysis of the X-chromosome SNVs were excluded. Family-reported relationships were genetically confirmed by pairwise genome-wide estimates of identity by descent (IBD) allele sharing using PLINK v1.07 software.[38]

Statistical analysis

Genome-wide tests of parametric linkage and association analysis. SNV genotype data (MAF$\geq 1\%$ from WGS) were available for a total of 451 study participants. Parametric linkage analysis was performed in 767 study participants (350 affected with ET, 101 unaffected, and 316 pedigree members with inferred genotypes) from 104 multiplex ET families. For the 316 pedigree members without WGS data, with the exception of gender, phenotype data was coded as missing. We used Pseudomarker[39] software to allow for joint linkage and linkage disequilibrium analysis. Analyses were restricted to variants with MAF $\geq 1\%$. Model-based analyses were carried out using an age-dependent penetrance model (Table 2) with disease allele frequency of 1%, under a dominant mode of inheritance. The age-dependent penetrance model (Table 2) is based on available prevalence data for ET across different age groups,[40,41] estimation of penetrance in affected subjects, and phenocopy rates across liability classes. Three age groups (≤ 40 years, $41-59$ years and ≥ 60 years) were used in the model and individuals were stratified based on age at onset (AAO) in affected subjects. A total of 7 liability classes were used in the model (Table 2). The Lander and Kruglyak threshold for genome-wide linkage was established as HLOD ≥ 3.6.[42] Correction for multiple testing in the joint linkage and association analysis was performed using Bonferroni-adjusted $p \leq 10^{-6}$.

Liability Class	Age group (years)	Genotype Specific Penetrance in Wildtype (P)[a]	Genotype Specific Penetrance in Heterozygous Mutation Carriers (P)[b]	Genotype Specific Penetrance in Homozygous Mutation Carriers (P)[b]
1: Fully penetrant	≤40	0.01	1	1
2: Fully Penetrant	41-59	0.02	1	1
3.Fully Penetrant	≥60	0.22	1	1
4: Incomplete penetrance	≤40	0.01	0.4	0.4
5: Incomplete penetrance	41−59	0.02	0.2	0.2
6: Incomplete penetrance	≥60	0.22	0.1	0.1
7: Incomplete penetrance	Unknown	0.5	0.5	0.5

Table 2: Age-dependent penetrance model—Dominant model.
[a] The probability of developing ET in individuals with wildtype genotype is equal to the phenocopy rate.
[b] P: Probability of ET given a particular genotype.

Collapsed Haplotype Pattern non-parametric linkage analysis. The CHP-NPL method[43,44] was also used to analyse families segregating ET using the same dataset. The 2 individuals with PD, 11 with dystonia and 7 whose tremor was not severe enough to meet criteria for ET were removed from CHP-NPL analyses. Only affected ET families were included in the CHP-NPL analysis. A total of 98 ET families and 703 individuals were included in the CHP-NPL analysis. CHP-NPL analysis of all variants in aggregate within a gene region regardless of the functional annotation. Annotation of gene regions was performed using Annovar. As suggested by Lander and Kruglyak,[42] we applied the most stringent threshold level, with a LOD score of ≥3.8.

Variant analysis of WGS data

Pseudomarker. To identify susceptibility variants, in linkage regions segregating with the ET phenotype, in families contributing to the linkage peaks on chromosomes 4q21. 8q13.3, 8q21.1, 16p13.3 and 17q21.31 we performed additional sequence analysis of WGS data in 9 ET families (A-I). Additional analyses included evaluation of SNV and indels, copy number variants (CNVs) and structural variants (SVs), and short tandem repeat (STR) expansions within linkage peaks.

SNVs and indels
Variant filtering, annotation and prioritization was performed using a previously described pipeline and reviewed as part of the clinical workflow for constitutional clinical sequencing (Precision Genomics Laboratory, Vagelos College of Physicians and Surgeons, Columbia University). Sample level variant calls and associated quality metrics (GT, DP, GQ, VQSLOD and SQR, DP Bin string) was performed followed by variant annotation (chromosome, position, reference allele, alternative allele, effect, gene and transcript) and annotation with external data (gnomad, Gerp, TraP, LIMBR, ClinVar, HGMD, RVIS and REVEL). Variants (coding) with allele frequencies of less than 1% or known

susceptibility variants with allele frequency <10% in the general population, were filtered using the Gnomad and in-house databases. Identified variants were assessed for phenotype match with ET. Variants were classified using the guidelines from the American College of Medical Genetics and Genomics (ACMG) and the Association of Molecular Pathology (AMP).[45] Variants were classified as Pathogenic, Likely Pathogenic and Variants of Uncertain Significance (VUS).

CNVs and SVs: Multisample CNV calling was performed from WGS data using the DRAGEN DNA pipeline. Multisample CNV calling in DRAGEN uses tangent normalized count files from WGS data and joint segmentation to increase the sensitivity of detection of CNV segments. For each copy number variable segment identified, the copy number genotype of each sample is outputted in a single VCF entry. The DRAGEN Structural Variant (SV) caller was used to call SVs from the WGS data and provides SV and indel calls >50bp.

Selecting rare or novel CNVs
Common variants were removed following comparison with the Database of Genomic Variants (DGV) and 1000 Genomes CNV calls, and using a criterion of 50% or more reciprocal overlap with population CNVs with 1% or higher frequency. BEDTools was used to identify called genic CNVs that overlapped with variants in databases.

Reducing false calls
To minimize false calls, rare genic CNV calls from each affected individual was used to query calls in affected and unaffected family members for the same or similar breakpoints. If the same CNV (consensus of the two tools) was present in affected individuals and absent from unaffected individuals it was included in the final list.

Annotation of CNV calls
Annotation of CNV calls was performed using variant effect predictor (VEP) which determines the effect of

the variant on genes, transcripts and protein sequences as well as regulatory regions population databases including the Database of Genomic Variants (DGV) and dbVar (National Center for biotechnology information), and literature evidence (OMIM, ClinVar, COSMIC, etc).

De novo CNV calling

De novo CNV calling was not performed as sequence data was not available from both parents. Trio families were not included in the analysis.

Repeat Expansion Detection: Repeat expansion detection from the WGS data was performed with Expansion Hunter[46] in the DRAGEN pipeline. Expansion Hunter performs sequence-graph based realignment of reads that originate inside and around each tandem repeat and genotypes the length of the repeat in each allele. Only repeat variants that deviated significantly from the reference genome (Human GRCh37/h19) were considered for further analysis.

To identify rare genic CNVs, SVs and repeat expansions segregating with ET in each family a family-based analysis was performed. The criteria that we used to define co-segregation is as follows: 1) the annotated CNV was present in all affected ET individuals and 2) absent from unaffected individuals within a family.

CHP-NPL analysis

To identify the additional contribution of rare variants to linkage signals in haplotype-based analysis, in genes with evidence of significant linkage (LOD≥3.8) identified by CHP-NPL analysis, we performed additional sequence analysis of WGS data in ET families. Additional analyses included evaluation of SNVs and indels. Variant filtering, annotation and prioritization was performed using the Varsome clinical platform.

Brain expression analysis

To investigate brain expression profiles of the identified candidate ET genes within the Pseudomarker linkage regions, we used the publicly available data from the United Kingdom Brain Expression Consortium (UKBEC) repository, which is based on tissue from 12 brain regions from 134 individuals free of neurodegenerative disorders analysed using the Affymetrix Exon 1.0 ST array (http://www.braineac.org/). The datasets used contain the information for SNPs and indels found within 1Mb of the transcription start site of the transcript (total span of 2Mb). Markers were restricted to those with good imputation quality ($R^2 > 0.5$) and MAF ≥5%.

Gene annotation and pathway analysis

Phenotype, molecular function, pathway and interaction data for genes identified in the analysis were obtained from Genecards Suite version 5.8.[47] Pathway analysis

was also performed using the reactome pathway knowledgebase version 79.[48]

Role of funding source

The funders had no role in study design, data collection, data analyses, interpretation, or writing of report.

Results

Data were collected and analysed between July 2015 and February 2021. The analysis pipelines used for Pseudomarker and CHP-NPL analyses in 104 ET families are summarized in Figure 1 and pedigrees are shown in Supplementary Figure 1.

The demographic and clinical characteristics of study participants included in the analyses are summarized in Table 1. A total of 451 subjects with WGS data from 104 ET families were included in the analyses. The mean age at onset in ET cases was 31.2 ±19.9 years. Of the 330 ET cases, 16.1% received a diagnosis of definite ET, 48.5% probable ET and 35.4% possible ET. In addition, there were 2 individuals with Parkinson's disease (PD), 11 with diagnoses of dystonia and 7 whose tremor was not severe enough to meet criteria for ET.

The mean age for all subjects was 60.2±17.1 years. The mean number of affected ET cases per family was 5.7±2.0, and the mean number of unaffected family members per family was 1.8 ±1.6. Eleven families (11.1%) reported Ashkenazi Jewish ancestry.

Joint parametric linkage and association analysis

We identified several significant (HLOD≥3.6) chromosomal regions linked to ET (Supplementary Figure 2; Table 3). Functional annotation of all significant loci was performed and we selected functionally relevant candidate genes that map to functionally relevant pathways (Table 3). All significant linkage regions identified with HLOD≥3.6, ranked by *p* value are provided as supplementary data (Supplementary Table 1). The 3-unit LOD support intervals for all significant (HLOD≥3.6) chromosomal regions linked to ET in Table 3 are provided in Supplementary Table 2. Further annotation of SNVs with max LOD scores in the support intervals using ENCODE and the UCSC Genome Browser are also provided in Supplementary Table 3.

The strongest ET linkage signal corresponding to chromosome 4q13.3, was observed for the SNV, rs10012100, located telomeric to Betacellulin (*BTC*), and ∼36.3 Kb upstream of the *BTC* transcription start site (rs10012100; HLOD=4.53; P_{joint}=1.1 × 10^{-5}). *BTC* is a member of the epidermal growth factor (*EGF*) family of proteins, a neurotrophic factor, involved in the EGFR-PI3K-AKT pathway which is disrupted in PD[49] and ET.[50]

A SNV located at chromosome 21q21.3, rs2831975, showed significant evidence of linkage (HLOD=4.31; P_{joint}=2.6 × 10^{-5}). The SNV is located centromeric
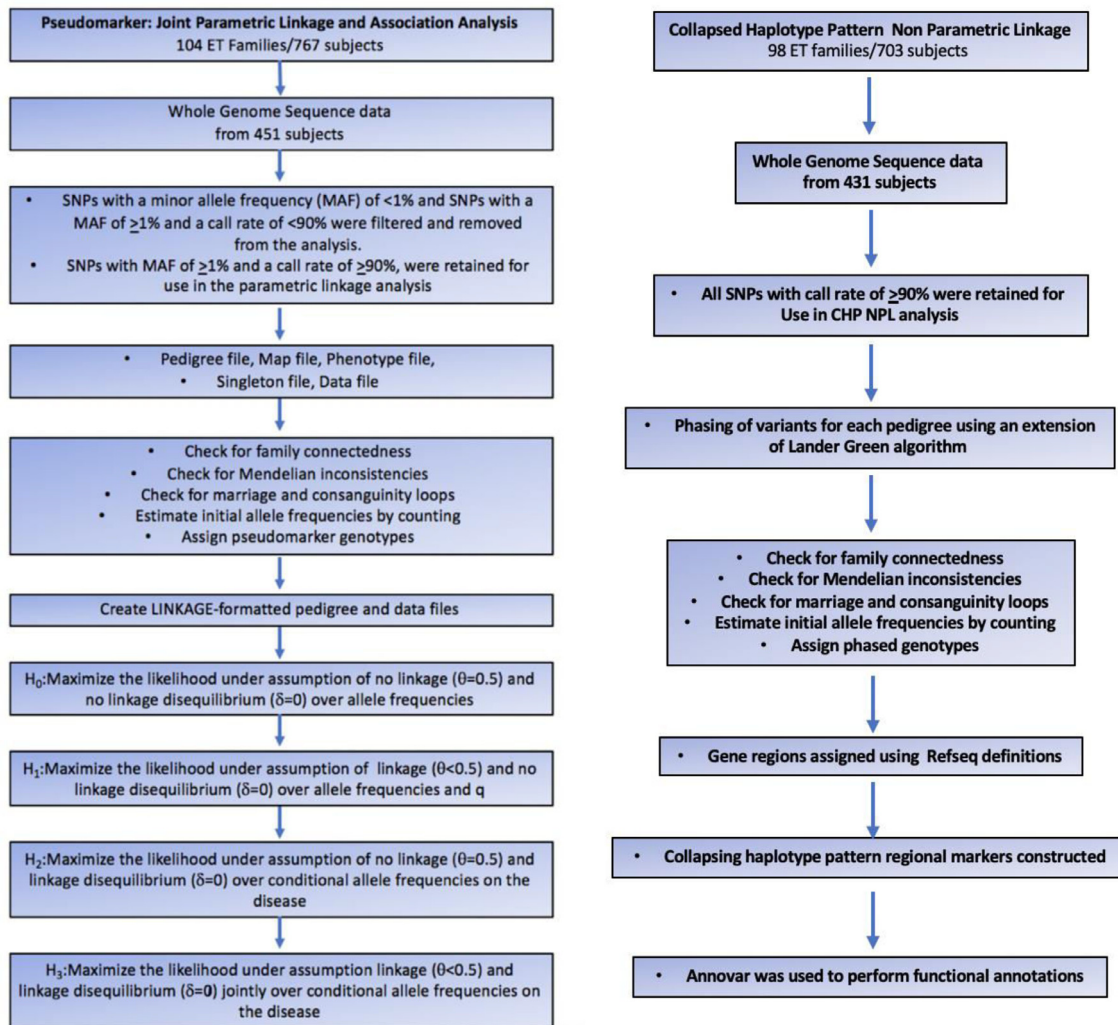
Figure 1. Workflow of Genome-Wide linkage scan using Pseudomarker and RV NPL in 104 ET families.

(~162.2Kb distal) to the N-6 Adenine-specific DNA methyltransferase 1 gene (*N6AMT1*). *N6AMT1* encodes a methyltransferase which may be involved in the methylation of release factor I during translation termination and is also involved in converting the toxin arsenic metabolite monomethylarsonous acid to the less toxic dimethylarsonic acid.[51] Among, other genes located in the same chromosomal region, the glutamate ionotropic receptor kainite type subunit 1 (*GRIK1*) and amyloid beta precursor protein (*APP*) gene are of particular interest based on function and association with neurological disease.

The linkage peak on chromosome 13q21.32 is driven by, rs56402633 (HLOD=4.21) and rs288791 (HLOD=4.05). The variants are proximal (~655.6 Kb) to the gene Protocadherin 9 (*PCDH9*). Under the dominant model, rs56402633, is significantly associated with ET (P_{joint}=3.0 × 10^{-6}). *PCHD9* encodes a member of

the protocadherin family, which mediate cell adhesion in neural tissues in the presence of calcium and may also be involved in signalling at neuronal synaptic junctions.[52]

On chromosome 8q13.3, a linkage signal was observed for an intronic variant (intron 2) within Eyes Absent Transcriptional Coactivator and Phosphatase 1 (*EYA1*) gene (rs4439163; HLOD=4.04). Results from the joint linkage and association analysis demonstrated that under the dominant model, rs4439163, is significantly associated with ET (P_{joint}=4.0 × 10^{-6}). A second linkage signal nearby at 8q21.1 with HLOD=3.66 (P_{joint}=1.3 × 10^{-4}) was also observed with the SNV, rs10097236, located in intron 12 of the gene, Staufen Double-Stranded RNA binding protein 2 (*STAU2*) gene. *STAU2* is a member of a family of double stranded RNA binding proteins that contains a microtubule binding domain that binds tubulin. A related family

Chr	SNV	bp	band	Gene[a]/nearest gene Intron/exon	Linkage HLOD	Linkage *p*-value	LD|Linkage *p*-value	LD|NoLinkage *p*-value	Linkage|LD *p*-value	LD+Linkage *p*-value
1	rs78261279	40805774	p34.2	Collagen type IX alpha 2 chain COL9A2	3.88	1.2×10^{-5}	0.745	0.058	$1.5 \times 10 \times 10^{-4}$	7.4×10^{-5}
4	rs10012100	75756056	q13.3	Betacellulin BTC	4.53	3.0×10^{-6}	0.352	0.591	4.0×10^{-6}	1.1×10^{-5}
4	rs13111888	77131294	q21.1	Scavenger receptor class B member 2 SCARB2 Intron 1	3.65	2.1×10^{-5}	0.8507	0.7045	4.4×10^{-5}	1.29×10^{-4}
8	rs7827299	72301916	q13.3	EYA transcriptional coactivator and phosphatase 1 EYA1	3.60	2.4×10^{-5}	0.0620	0.9268	8.0×10^{-6}	2.6×10^{-5}
8	rs372304696	72320706	q13.3	EYA transcriptional coactivator and phosphatase 1 EYA1	3.70	1.8×10^{-5}	0.1871	0.1975	3.5×10^{-5}	4.9×10^{-5}
8	rs4439163	72333781	q13.3	EYA transcriptional coactivator and phosphatase 1 EYA1	4.04	8.0×10^{-6}	0.0219	0.6005	1.0×10^{-6}	4.0×10^{-6}
8	rs10097236	74436131	q21.1	Staufen double-stranded RNA binding protein 2 STAU2 Intron 12	3.66	2.0×10^{-5}	0.9164	0.0761	2.2×10^{-4}	1.3×10^{-4}
13	rs56402633	68460037	q21.32	Protocadherin 9 PCDH9	4.21	5.0×10^{-6}	0.021	0.06	4.0×10^{-6}	3.0×10^{-6}
13	rs288791	68460037	q21.32	Protocadherin 9 PCDH9	4.05	8.0×10^{-6}	0.624	0.209	3.2×10^{-5}	4.7×10^{-5}
13	rs9538356	59832966	q21.2	Diaphanous related formin 3 DIAPH3	3.68	1.9×10^{-5}	0.847	0.908	3.8×10^{-5}	1.2×10^{-4}
14	rs4624102	78562248	q24.3	Neurexin 3 NRXN3	3.65	2.1×10^{-5}	0.93	0.209	9.5×10^{-5}	1.3×10^{-4}
16	rs8051198	6541644	p13.3	RNA binding fox-1 homolog RBFOX1 Intron 2	4.02	8×10^{-6}	0.4298	0.2807	2.3×10^{-5}	4.1×10^{-5}
16	rs114400470	1044241	p13.3	SRY-box transcription factor 8 SOX8	3.8	1.4×10^{-5}	0.504	0.528	2.8×10^{-5}	7.4×10^{-5}
17	rs8076152	43995932	q21.31	Microtubule associated protein tau MAPT Intron 1	3.99	9×10^{-6}	0.4263	0.5480	1.6×10^{-5}	4.4×10^{-5}
21	rs2831975	30086239	q21.3	N-6 adenine-specific DNA methyltransferase 1 N6AMT1	4.31	4.0×10^{-6}	0.663	0.67	8×10^{-6}	2.6×10^{-5}

Table 3: **Top significant candidate chromosome regions with HLOD≥3.6 in the pseudomarker analysis in 104 ET families.**

[a] Hugo Gene Nomenclature Committee (HUGO) approved gene name and symbol; HLOD: Heterogeneity logarithm of odds score; LD|Linkage: Linkage disequilibrium (association) given linkage; LD|NoLinkage: Linkage disequilibrium (association) given no linkage; Linkage|LD: Linkage given linkage disequilibrium; LD+Linkage: Joint linkage and association.

member, *STAU1*, has been implicated in neurodegeneration and hyperactive mTOR.[53]

The 16p13.3 linkage region (HLOD=4.02; P_{joint} = 4.1×10^{-5}) also yielded strong evidence for linkage at SNV, rs8051198, located in intron 2 of the RNA Binding Fox-1 Homolog 1 (*RBFOX1*) gene. *RBFOX1* belongs to the FOX1 family of RNA-binding proteins. FOX1 proteins bind the C-terminus of ataxin-2 and may contribute to disease pathophysiology of spinocerebellar ataxia 2 (*SCA2*).[54,55] The 4 aminobutyrate aminotransferase (*ABAT*) gene is also located in the same chromosomal region. *ABAT* is responsible for the catabolism of gamma aminobutyric acid (GABA), and a disturbance of the GABAergic system has been strongly implicated in ET.[56−58]

The linkage peak on chromosome 17q21.31 (HLOD=3.99; P_{joint} =4.4×10^{-5}) is driven by an intronic SNV, rs8076152, located in intron 1 of the microtubule-associated protein tau (*MAPT*) gene. In addition to *MAPT*, which is associated with several neurodegenerative disorders,[59] this region contains other genes that are plausible candidates (e.g. *KANSL1* and *STH*), many of which are highly expressed in different brain regions, including the cerebellum.

Additional significant linkage signals were also observed on chromosomes 1 (rs78261279; HLOD=3.88, nearest gene: Collagen type IX alpha 2 chain (*COL9A2*)), 16 (rs114400470; HLOD=3.8, nearest gene: SRY-box transcription factor 8 (*SOX8*)), 13 (rs9538356; HLOD=3.68, nearest gene: Diaphanous related formin 3 (*DIAPH3*)), 14 (rs4624102; HLOD=3.65, nearest gene: Neurexin 3 (*NRXN3*)) and 4 (rs13111888; HLOD=3.65, *SCARB2* intron 1) (Table 3).

FASET families contributing to significant parametric linkage in the pseudomarker analysis

The highest LOD score for each family in the pseudomarker analysis was determined to identify families contributing to significant linkage regions (Supplementary Table 4). We then performed further analysis of WGS data to identify causal or risk variants in these families.

SNV and indel analysis in families contributing to significant linkage regions.

In one family, Family F, that contributed significant linkage to Chr16p13.3 (*RBFOX1*) (Supplementary Table 4), we identified a heterozygous canonical splice acceptor variant in exon 2 (ENST00000547372; c.4-2A>G), which was present in affected individuals and absent from unaffected individuals with available DNA (Supplementary Figure 3). This variant is extremely rare in the gnomAD population database (v2.1.1) with an allele frequency of 7.4×10^{-6} (1/135582 heterozygotes and 0 homozygotes) indicating it is not a common benign variant. The variant has not

been reported previously in the literature or clinical databases. Several *in silico* prediction algorithms, including splice prediction tools, indicate that the variant is predicted to disrupt splicing and is damaging or deleterious to the protein. These tools include BayesDel (Damaging, rank score 0.7802), Dann (score 0.9888), Eigen (pathogenic, score 0.9989), FATHMM-MKL (Damaging, score 0.9661), dbscSNV (deleterious, score 0.76) and RF (deleterious, score 0.76). Classification of the variant according to the American College of Medical Genetics (ACMG) criteria indicates that this variant meets criteria as a likely pathogenic variant.

We did not identify rare coding SNVs or indels in any other genes, that segregate in families contributing to significant linkage regions.

However, annotation of the 3-unit LOD support intervals for significant regions reported in Table 3 (Supplementary Table 2) and analysis in families contributing to significant linkage regions shows that significant SNVs identified by Pseudomarker are located in regulatory regions that impact transcription factor binding sites or chromatin state (Supplementary Table 3). For example, in families contributing to significant linkage in intron 2 of *EYA1*, the marker at chr8:72333781 (max LOD) is located in several predicted transcription factor binding sites (Jasper Core 22) including *NEUROD1, PTF1a, NEUROD2, ATOH1, PKNOX2, TGIF1, TGIF2LX, TWIST1, NEUROG2* and *HAND2*. These transcription factors play an important role during embryonic and neural development. The transcription factor *NEUROG2*, specifies neuronal fate on ectodermal cells and is expressed in neural progenitor cells within the developing central and peripheral nervous systems and also plays a role in the differentiation and survival of midbrain dopaminergic neurons.

In families contributing to significant linkage at chr17q21.31 (*MAPT*), we identified the heterozygous missense variant, NM_001007532.3, c.20A>G (p.Q7R) in exon 1 of the Saitohin (*STH*) gene (nested within MAPT) which was present in affected individuals and absent from unaffected individuals with available DNA (Supplementary Figure 3) in one family (Family F) and in 2/3 affecteds with available DNA from a second family (Family E; *data not shown*). The *STH* Q7R has previously been reported as a risk factor for neurodegenerative disease including Parkinson's disease and Alzheimer's disease.

CNV/SV and repeat expansion analysis in families contributing to significant linkage regions.

CNV/SV and repeat expansions were not identified in any genes in families contributing to significant linkage regions.

CHP non-parametric linkage analysis

CHP-NPL analysis identified fifteen genes with evidence of significant linkage (LOD≥3.8). These were Tubulin beta 2A class IIi (*TUBB2A*) (LOD=7.42,

$p=5.0 \times 10^{-9}$), VPS33B late endosome and lysosome associated (*VPS33B*) (LOD=5.74, $p=2.73 \times 10^{-7}$), STEAP family member 1B (*STEAP1B*) (LOD=4.92, $p=1.96 \times 10^{-6}$), Serine peptidase inhibitor Kazal type 5 (*SPINK5*) (LOD=4.90, $p=2.06 \times 10^{-6}$), Zinc finger RANBP2-type containing 1 (*ZRANB1*) (LOD=4.87, $p=2.16 \times 10^{-6}$), TBC1 domain family member 3C (*TBC1D3C*) (LOD=4.78, $p=2.69 \times 10^{-6}$), Pyruvate dehydrogenase phosphatase regulatory subunit (*PDPR*) (LOD=4.75, $p=2.91 \times 10^{-6}$), Neuropeptide Y receptor Y4 (*NPY4R*) (LOD=4.65, $p=3.7 \times 10^{-6}$), ETS proto-oncogene 2, transcription factor (*ETS2*) (LOD=4.63, $p=3.84 \times 10^{-6}$), Zinc finger protein 736 (*ZNF736*) (LOD=4.59, $p=4.32 \times 10^{-6}$), Spermatogenesis associated 21 (*SPATA21*) (LOD=4.36, $p=7.45 \times 10^{-6}$), ADP ribosylation factor like GTPase 17A (*ARL17A*) (LOD=4.12, $p=1.32 \times 10^{-5}$), PZP alpha-2-macroglobulin like (*PZP*) (LOD=3.99, $p=1.83 \times 10^{-5}$), BLK proto-oncogene, Src family tyrosine kinase (*BLK*) (LOD=3.98, $p=1.85 \times 10^{-5}$), and YJU2 splicing factor homolog (*YJU2/CCDC94*) (LOD=3.87, $p=2.42 \times 10^{-5}$) (Table 4). None of the genes that reached the significance threshold have been previously associated with ET. However, nominal significance was observed for 3 genes also identified in the Pseudomarker analysis. The three genes

include *EYA1* (Pseudomarker HLOD =4.04; CHP-NPL: LOD score=1.41, $p=0.011$), in addition to two genes, Myoferlin (*MYOF*) (Pseudomarker HLOD=3.07; CHP-NPL: LOD score=1.30, $p=0.015$) and Telomerase associated protein 1 (*TEP1*) (Pseudomarker HLOD=3.45; CHP-NPL: LOD score=1.34, $p=0.013$, which did not surpass the threshold level of significance (HLOD$\geq$3.6) (*data not shown*).

Of the genes identified in the CHP-NPL analysis several have been previously implicated in neurological disease (e.g. *TUBB2A*),[60,61] or interact with known PD disease genes (e.g., TBC1 domain family member 3C (*TBC1D3C*), ADP ribosylation factor like GTPase 17A (*ARL17A*) and Leucine rich repeat kinase 2 (*LRRK2*)) or Alzheimer's disease genes (e.g., PZP alpha-2-macroglobulin like (*PZP*) and *Sortilin related receptor 1* (*SORL1*)) (Supplementary Table 5). As observed in the pseudomarker analysis we also observed significant linkage to genes that cluster in ROS and DNA damage repair pathways (*PDPR*,[62] *STEAP1B* and *CCDC94*[63]), neurogenesis and cortical development pathways (*TUBB2A*[64] and *TBC1D3*[65]), lysosomal/endosomal and protein metabolism pathways (*VPS33B*[66], *ZRANB1*[67] and *ARL17A*), and EGFR-PI3K-AKT and ERK signalling (*VPS33B*[66], *ETS2*[69] and *BLK*). Significantly, *ARL17A* is

Chr	band	Gene name and symbol[*]	Linkage LOD	Linkage *p*-value
6	p25.2	Tubulin beta 2A class IIa *TUBB2A*	7.42	5.00×10^{-9}
16	q26.1	VPS33B late endosome and lysosome associated *VPS33B*	5.74	2.73×10^{-7}
7	p15.3	STEAP family member 1B *STEAP1B*	4.92	1.96×10^{-6}
5	q32	Serine peptidase inhibitor Kazal type 5 *SPINK5*	4.90	2.06×10^{-6}
10	q26.13	Zinc finger RANBP2-type containing 1 *ZRANB1*	4.87	2.16×10^{-6}
17	q12	TBC1 domain family member 3C *TBC1D3C*	4.78	2.69×10^{-6}
16	q22.1	Pyruvate dehydrogenase phosphatase regulatory subunit *PDPR*	4.75	2.91×10^{-6}
10	q11.22	Neuropeptide Y receptor Y4 *NPY4R*	4.65	3.70×10^{-6}
21	q22.2	*ETS proto-oncogene 2, transcription factor* *ETS2*	4.63	3.84×10^{-6}
7	q11.21	*ZNF736*	4.59	4.32×10^{-6}
1	p36.13	*SPATA21*	4.36	7.45×10^{-6}
17	q21.31	*ARL17A*	4.12	1.32×10^{-5}
12	p13.31	*PZP*	3.99	1.83×10^{-5}
8	p23.1	*BLK*	3.98	1.85×10^{-5}
19	p13.3	*CCDC94*	3.87	2.42×10^{-5}

Table 4: **Significant genes in CHP-NPL analysis with LOD$\geq$3.8 in 104 ET families.**
*Hugo Gene Nomenclature Committee (HUGO) approved gene name and symbol.

located on chromosome 17q21 within the *MAPT* haplotype region and significant linkage to *MAPT* was identified in the pseudomarker analysis (HLOD=3.99).

Bioinformatic evaluation and frequencies of analyzed rare (MAF<1%) coding variants within genes with evidence of significant linkage (LOD≥3.8) from the CHP-NPL analysis is shown in Supplementary Table 6. Rare coding variants identified in ET families with enhanced minor RV allele sharing in affected individuals are provided as Supplementary data.

Brain expression analysis

Results from the analysis using the Brain Almanac repository (Supplemental data) showed that ET candidate genes displayed brain region-specific expression patterns and high expression in several brain regions including the cerebellum (Supplementary Figure 4).

Pathway analysis

Pathway analysis of significant genes identified from the Pseudomarker and CHP-NPL analysis was performed using Genecards Suite version 5.8[47] and the reactome pathway knowledgebase version 79.[48] An overrepresentation analysis (a hypergeometric distribution test) was used to determine whether certain reactome pathways were over-represented (enriched) in the submitted data from significant genes in the pseudomarker analysis and from the CHP-NPL analysis (Supplementary Data). None of the pathways were significant after correction by FDR, however we did observe overrepresentation in the following pathways for significant genes identified in the Pseudomarker analysis including: 1) ROS and DNA repair: nuclear receptor transcription pathway (R-HSA-383280), Defective HDR through Homologous Recombination (HRR) due to Partner and localizer of BRCA2 (PALB2) loss of function (R-HSA-9701193), Defective HDR through Homologous Recombination (HRR) due to PALB2 loss of BRCA1 DNA repair associated (BRCA1) binding function (R-HSA-9704331), Defective HDR through Homologous Recombination (HRR) due to PALB2 loss of BRCA2 DNA repair associated (BRCA2)/RAD51 recombinase (RAD51)/RAD51 paralog C (RAD51C) binding function (R-HSA-9704646), ROS and RNS production (R-HSA-1222556) 2) EGFR-PIK3-AKT signalling: Growth factor receptor bound protein 2 (GRB2) events in EGFR signalling (R-HSA-179812), EGFR interacts with phospholipase C-gamma (R-HSA-212718), SHC adaptor protein 1 (SHC1) events in EGFR signalling (R-HSA-1250347), PI3K events in erb-b2 receptor tyrosine kinase 4 (ERBB4) signalling (R-HSA-1250342), PI3K events in ERBB2 signalling (R-HSA-1963642), Met proto-oncogene, receptor tyrosine kinase (MET) activates PI3K/AKT signalling (R-HSA-8851907), negative regulation of the PI3K/AKT network (R-HSA-199418),

PI3K/AKT signalling in cancer (R-HSA-2219528), PI5P, Protein phosophatase 2 phosphatase activator (PTPA), and Immediate early response 3 (IER3) regulate PI3K/ AKT signalling (R-HSA-681158), PIP3 activates AKT signalling (R-HSA-1257604), 3) GABAergic signalling: Activation of GABAB receptors (R-HSA-991365), GABAB receptor activation (R-HSA-977444), GABA receptor activation (R-HSA-977443)and 4) RNA binding and regulation of RNA processes: Regulation of PTEN mRNA translation (R-HSA-8943723), rRNA modification in the mitochondrion (R-HSA-6793080), FGFR2 alternative splicing (R-HSA-6803529), RNA polymerase II transcription (R-HSA-73857).

Discussion

Linkage and association analyses in 104 multi-generational ET families with multiple family members affected by ET identified several novel regions with suggestive linkage and association to ET. These regions contain functionally relevant candidate ET genes. We also observed possible overlap of loci identified from the Pseudomarker analysis (Supplementary Table 1) with previously reported linkage loci, *ETM2* (Chr2p25-22) and *ETM5* (Chr11q14).

Among the gene regions identified in the Pseudomarker analysis, causal or risk variants are located in regulatory regions that may impact transcription factor binding sites or chromatin state during development. Our analysis suggests that genetic factors impacting neurodevelopment may be a risk factor for ET.

Four genes (*BTC, COL9A2, DIAPH3* and *SOX8*) identified also are involved in the EGFR-PI3K-AKT or ERK-mediated signal transduction pathways. The major functions of the regulatory proteins in these pathways includes cell survival, motility, transcription, metabolism and progression of cell cycle.[50] Disruption of EGFR-PI3K-AKT or ERK-mediated signalling contributes to the pathogenesis of several neurodegenerative diseases including ET.[49,50] *BTC* is a member of the epidermal growth factor (*EGF*) family of proteins, a neurotrophic factor, involved in the EGF/EGF-Receptor pathway. The leucine rich repeat and Ig domain containing 1 (*LINGO-1*) gene, a risk factor for ET identified from GWAS studies,[28] can bind EGFR and induce downregulation of the activity of EGFR-PI3K-AKT signalling pathway, leading to decreased Purkinje cell survival in the cerebellum. Increased cerebellar LINGO-1 expression and elongated LINGO-1-positive ponceau processes have been observed in ET brains, suggesting a role for this pathway in ET disease pathogenesis.[70] A similar mechanism may involve genetic variants in EGFR in ET patients leading to downregulation of the activity of EGFR-PI3K-AKT signalling pathway and Purkinje cell death. In addition to *BTC*, linkage signals at three genes (*COL9A2, DIAPH3* and *SOX8*) were also identified with a known function in ERK signalling

pathways. Development of therapeutics targeting activation of the EGFR-PI3K-AKT pathway or inhibition of the ERK pathway may be beneficial in treatment of ET.

Ageing is a leading risk factor for neurodegenerative disease and cancer.[71] Several studies have suggested that several major signalling pathways and molecular targets are modulated in aging including oxidative stress and DNA repair. ROS cause oxidative damage in cellular macromolecules, including DNA, proteins and lipids leading to decreased biochemical and physiological function though aging.[71] The cerebellum is particularly vulnerable to disorders of DNA repair, and ataxia and tremor are clinical features often observed in these disorders. Numerous studies, from clinical to neuroimaging to pathological, provide evidence that the cerebellum is of prime importance in the disease pathophysiology of ET.[8−10] In our study, significant linkage peaks were identified within or near to four genes, *N6AMT1*, *EYA1*, *SCARB2* and *MAPT* that may contribute to increased ROS and defects in DNA repair. *N6AMT1* may play a role in the modulation of arsenic-induced toxicity by mediating the conversion of monomethylarsonous acid to the less toxic dimethylarsonic acid.[51] Arsenic, one of the most common environmental pollutants, is a known toxic metalloid that contributes to ROS production, DNA damage and mitochondrial dysfunction.[72] *EYA1*, a member of the EYA class of proteins is critical for Shh-dependent hindbrain growth and development[73] and mediates symmetric cell division of cerebellar granule cell precursors.[74] *EYA1* also plays a role in DNA repair. *EYA1* can dephosphorylate the c-terminal phosphotyrosine 142 (pY142) of H2AX, a histone protein and an essential regulator of the DNA damage response.[75,76] *SCARB2*, which acts as a lysosomal receptor for glucocerebrosidase (*GBA*) targeting, and plays a role in α-synuclein aggregation, may also contribute to ROS and oxidative stress. More recent studies have proposed that protein aggregates of α-synuclein can directly cause DNA breaks[77] and DNA repair defects.[77] A similar mechanism may also involve the *MAPT* gene, which was also identified in the current study. *MAPT* encodes a cytoskeletal protein, tau, which interacts with microtubules and has a role in neuron morphogenesis, axonal transport and is a major misfolded aggregated protein found in Alzheimer's disease (AD) and frontotemporal dementia and Parkinsonism linked to chromosome 17.[59] Studies suggest tau can bind DNA, is recruited to the nucleus where it binds to chromatin during heat stress and plays a role in genome stability. In animal models of genetic tauopathy, significantly higher levels of aneuploidy were observed in mice expressing human tau carrying the p. P301L or P301S pathogenic variants respectively, compared to control mice.[78] Several lines of evidence also point to abnormal tau biology in ET. Although there have been inconsistent reports of genetic association of the *MAPT* H1 haplotype with ET,[79−81] which may reflect sampling issues or clinical heterogeneity, neurofibrillary tangle (NFT) positive neurons and a higher tau burden has been reported in post mortem ET studies.[82,83] In two of three families contributing to significant linkage at chr17q21.31 (*MAPT*), we identified the heterozygous missense variant, NM_001007532.3, c.20A>G (p.Q7R) in exon 1 of the Saitohin (*STH*) gene (nested within MAPT) The *STH* Q7R risk variant has previously been reported as a risk factor for neurodegenerative disease including Parkinson's disease and Alzheimer's disease. *STH* is involved in the positive regulation of mRNA splicing via the spliceosome and located in the nucleus and perinuclear region of the cytoplasm and may play a role in alternative splicing of *MAPT* and an increase in 4R/3R MAPT ratio.

Other linkage signals identified in the current study are implicated in the GABAergic system and in RNA binding and RNA processing. Linkage signals at two genes, *PCDH9* and *NRXN3*, encode cell adhesion molecules that are members of the Protocadherin and Neurexin gene families respectively. Pathogenic variants in *NRXN3* and *PCDH9* have been identified in patients with autism spectrum disorder (ASD)[52] and the GABAergic system is implicated in the aetiology of ASD. Similarly, a disturbance of the GABAergic system has been strongly implicated in ET.[56−58]

STAU2 and *RBFOX1* belong to a class of RNA binding proteins (RBPs) that are involved in the regulation of various RNA processes such as RNA stability, alternative pre-mRNA splicing, mRNA decay, translocation, post-translational nucleotide modifications and RNA localization.[84] The importance of RBPs and posttranscriptional regulation is highlighted by the severe neuropathologies caused by defects in RBPs, such as mental retardation or epilepsy, and motor defects such as ALS.[85−88] *STAU2* mediates the degradation of mRNA containing complex secondary structures in their 3' untranslated region (UTR) through a pathway known as Staufen-mediated mRNA decay.[89] In the brain, *STAU2* is an RNA binding protein that is involved in regulation of neuronal target mRNAs and dendritic spine morphogenesis and function.[90] In a $Stau2$ downregulation ($Stau^{GT}$) cerebellar Purkinje cell mouse model, an increase of glutamate receptor ionotropic delta subunit 2 (GLUD2) in Purkinje cells was observed when animals performed physical activity (wheel running) compared to age-matched wildtype control mice.[90] Furthermore, $Stau^{GT}$ mice also showed lower motor coordination abilities but increased motor learning capacity in the rotarod test.[90] The importance of GLUD2 as a key component of the Purkinje cell postsynapse has been previously reported. GLUD2 knockout mouse models have prominent motor dyscoordination and cerebellar ataxia[91,92] and mice with GLUD2 insufficiency and climbing fiber-Purkinje cell synaptic pruning deficits develop ET-like tremor.[93] *RBFOX1* is an *Rbfox* family member. *Rbfox* RBPs are expressed in adult

mammalian brain and are required for proper brain development and function.[94] Studies in mice and humans have implicated *Rbfox1/RBFOX1* in autism, neuronal excitation and epilepsy. Mouse models demonstrate a role for *Rbfox1* in neuronal migration during cortical development[55] and in the adult zebrafish brain, *Rbfox1l* shows restricted expression in the dorsal telencephalon and cerebellum in the Purkinje cell layer.[94] In yeast 2 hybrid assays, Rbfox1 was shown to interact with Ataxin-2, the protein mutated in spinocerebellar ataxia 2 (SCA2),[95] suggesting a role for Rbfox proteins in cerebellar development, function and motor movements.

In one Family (Family F), contributing to the linkage peaks on chromosome 16p13.3, we identified a likely pathogenic heterozygous canonical splice acceptor variant in exon 2 of *RBFOX1* (ENST00000547372; c.4-2A>G), that co-segregated with the ET phenotype in the family. Further studies will be needed to determine the functional significance of this variant in ET. Rare (MAF<1%) coding variants (SNV/Indels, CNV/SVs or repeat expansions) were not identified in any of the other 8 families analyzed that contribute to the linkage peaks on chromosomes 4q21.1, 8q13.3, 8q21.1, 16p13.3 and 17q21.31. Further sequence analysis of susceptibility variants and variants in non-coding regions in these families may help pinpoint ET genes in the regions.

Of the significant genes (LOD≥3.8) identified in the CHP-NPL analysis, many of the genes impact the same pathways identified using pseudomarker analysis. These genes cluster in ROS and DNA damage repair pathways (*PDPR*,[62] *STEAP1B* and *CCDC94*[63]), neurogenesis and cortical development pathways (*TUBB2A*[64] and *TBC1D3*[65]), lysosomal/endosomal and protein metabolism pathways (*VPS33B*,[66] *ZRANB1*[67] and *ARL17A*), and EGFR-PI3K-AKT and ERK signalling (*VPS33B*,[68] *ETS2*[69] and *BLK*) providing further evidence for the involvement of these pathways in ET disease pathogenesis.

We acknowledge potential limitations of the study. Firstly, our study represents a discovery stage one cohort and we did not include an independent stage 2 replication cohort. This was due in part to the limitations in recruitment and meticulous phenotyping, costs associated with WGS and the genetic heterogeneity of ET. Future large scale genetic analyses of WGS datasets (e.g. NIHs All of Us) or of other neurological datasets with a tremor phenotype (e.g. the Michael J. Fox Foundation Global Genetic Parkinson's Disease Study Group[96]) may be the most effective way of replicating findings. Secondly, pseudomarker and CHP-NPL do not deal with population stratification. However, one of the advantages of family-based studies is their robustness to population stratification. To limit population stratification in genetic analyses, we carefully sampled pedigrees and restricted analysis to white participants with European and N. American ancestry.

A strength of the study is the identification of linkage to genes implicated in the EGFR-PI3K-AKT signalling and ERK pathways in ET. Therapeutic strategies targeting these pathways may offer potential treatments for ET patients. Drug repurposing of the human anti-LINGO-1 antibody Li81 (opicinumab, Phase 2 for MS, ClinicalTrials.gov, NCT03222973), which blocks LINGO-1 function and is upstream of the EGFR-PI3K-AKT signalling pathway offers an opportunity to help accelerate the search for a treatment for ET patients.

In summary, our study provides evidence for a possible overlap in the genetic architecture of ET, other neurological diseases, cancer and ageing. The possible involvement of EGFR-PI3K-AKT signalling and ERK pathways in ET paves the way for functional studies and development of therapeutic strategies targeting these pathways.

Contributors

Data sharing statement

Declaration of interests

Acknowledgements

Supplementary materials

References

1 Louis ED. Clinical practice. Essential tremor. *N Engl J Med.* 2001;345(12):887–891.

2 Louis ED. The primary type of tremor in essential tremor is kinetic rather than postural: cross-sectional observation of tremor phenomenology in 369 cases. *Eur J Neurol.* 2013;20(4):725–727.

3 Louis ED, LSt Dure, Pullman S. Essential tremor in childhood: a series of nineteen cases. *Mov Disord.* 2001;16(5):921–923.

4 Louis ED, Ferreira JJ. How common is the most common adult movement disorder? Update on the worldwide prevalence of essential tremor. *Mov Disord.* 2010;25(5):534–541.

5 Louis ED, M M. How common is essential tremor? Update on the worldwide prevalence of essential tremor. *Tremor Other Hyperkinet Mov (N Y).* 2021.

6 Clark LN, Louis ED. Essential tremor. *Handb Clin Neurol.* 2018;147:229–239.

7 Louis ED. The essential tremors: evolving concepts of a family of diseases. *Front Neurol.* 2021;12:650601.

8 Louis ED, Faust PL. Essential tremor pathology: neurodegeneration and reorganization of neuronal connections. *Nat Rev Neurol.* 2020;16(2):69–83.

9 Louis ED, Faust PL. Essential tremor within the broader context of other forms of cerebellar degeneration. *Cerebellum.* 2020;19(6):879–896.

10 Louis ED. De Sedibus et Causis Morborum: is essential tremor a primary disease of the cerebellum? *Cerebellum.* 2016;15(3):233–234.

11 Tanner CM, Goldman SM, Lyons KE, et al. Essential tremor in twins: an assessment of genetic vs environmental determinants of etiology. *Neurology.* 2001;57(8):1389–1391.

12 Lorenz D, Frederiksen H, Moises H, Kopper F, Deuschl G, Christensen K. High concordance for essential tremor in monozygotic twins of old age. *Neurology.* 2004;62(2):208–211.

13 Bain PG, Findley LJ, Thompson PD, et al. A study of hereditary essential tremor. *Brain.* 1994;117(Pt 4):805–824.

14 Louis ED, Ford B, Frucht S, Rabinowitz D, Ottman R. Evidence for familial aggregation of tremor in normal individuals. *Neurology.* 2001;57(1):110–114.

15 Gulcher JR, Jonsson P, Kong A, et al. Mapping of a familial essential tremor gene, FET1, to chromosome 3q13. *Nat Genet.* 1997;17(1):84–87.

16 Higgins JJ, Pho LT, Nee LE. A gene (ETM) for essential tremor maps to chromosome 2p22-p25. *Mov Disord.* 1997;12(6):859–864.

17 Kovach MJ, Ruiz J, Kimonis K, et al. Genetic heterogeneity in autosomal dominant essential tremor. *Genet Med.* 2001;3(3):197–199.

18 Shatunov A, Sambuughin N, Jankovic J, et al. Genomewide scans in North American families reveal genetic linkage of essential tremor to a region on chromosome 6p23. *Brain.* 2006;129(Pt 9):2318–2331.

19 Hicks JE, Konidari I, Scott BL, et al. Linkage of familial essential tremor to chromosome 5q35. *Mov Disord.* 2016;31(7):1059–1062.

20 Illarioshkin SN, Rakhmonov RA, Ivanova-Smolenskaia IA, et al. [Molecular genetic analysis of essential tremor]. *Genetika.* 2002;38(12):1704–1709.

21 Lucotte G, Lagarde JP, Funalot B, Sokoloff P. Linkage with the Ser9Gly DRD3 polymorphism in essential tremor families. *Clin Genet.* 2006;69(5):437–440.

22 Merner ND, Girard SL, Catoire H, et al. Exome sequencing identifies FUS as a cause of essential tremor. *Am J Hum Genet.* 2012;91(2):313–319.

23 Parmalee N, Mirzozoda K, Kisselev S, et al. Genetic analysis of the FUS/TLS gene in essential tremor. *Eur J Neurol.* 2013;20(3):534–539.

24 Unal Gulsuner H, Gulsuner S, Mercan FN, et al. Mitochondrial serine protease HTRA2 p.G399S in a kindred with essential tremor and Parkinson disease. *Proc Natl Acad Sci U S A.* 2014;111(51):18285–18290.

25 Liu X, Hernandez N, Kisselev S, et al. Identification of candidate genes for familial early-onset essential tremor. *Eur J Hum Genet.* 2016;24(7):1009–1015.

26 Sanchez E, Bergareche A, Krebs CE, et al. SORT1 mutation resulting in sortilin deficiency and p75(NTR) upregulation in a family with essential tremor. *ASN Neuro.* 2015;7(4).

27 Bergareche A, Bednarz M, Sanchez E, et al. SCN4A pore mutation pathogenetically contributes to autosomal dominant essential tremor and may increase susceptibility to epilepsy. *Hum Mol Genet.* 2015;24(24):7111–7120.

28 Stefansson H, Steinberg S, Petursson H, et al. Variant in the sequence of the LINGO1 gene confers risk of essential tremor. *Nat Genet.* 2009;41(3):277–279.

29 Thier S, Lorenz D, Nothnagel M, et al. Polymorphisms in the glial glutamate transporter SLC1A2 are associated with essential tremor. *Neurology.* 2012;79(3):243–248.

30 Muller SH, Girard SL, Hopfner F, et al. Genome-wide association study in essential tremor identifies three new loci. *Brain.* 2016;139(Pt 12):3163–3169.

31 Odgerel Z, Sonti S, Hernandez N, et al. Whole genome sequencing and rare variant analysis in essential tremor families. *PLoS One.* 2019;14(8):e0220512.

32 Louis ED, Ottman R, Ford B, et al. The Washington Heights-Inwood Genetic Study of Essential Tremor: methodologic issues in essential-tremor research. *Neuroepidemiology.* 1997;16(3):124–133.

33 Amlang CJ, Trujillo Diaz D, Louis ED. Essential tremor as a "waste basket" diagnosis: diagnosing essential tremor remains a challenge. *Front Neurol.* 2020;11:172.

34 Deuschl G, Bain P, Brin M. Consensus statement of the movement disorder society on tremor. Ad Hoc scientific committee. *Mov Disord.* 1998;13(suppl 3):2–23.

35 Bhatia KP, Bain P, Bajaj N, et al. Consensus Statement on the classification of tremors. from the task force on tremor of the International Parkinson and Movement Disorder Society. *Mov Disord.* 2018;33(1):75–87.

36 Li H, Durbin R. Fast and accurate short read alignment with Burrows-Wheeler transform. *Bioinformatics.* 2009;25(14):1754–1760.

37 Van der Auwera GA, O'Connor BD. *Genomics in the cloud:using Docker, GATK and WDL in Terra.* 1st Ed. O'Reilly Media; 2020.

38 Purcell S, Neale B, Todd-Brown K, et al. PLINK: a tool set for whole-genome association and population-based linkage analyses. *Am J Hum Genet.* 2007;81(3):559–575.

39 Gertz EM, Hiekkalinna T, Digabel SL, Audet C, Terwilliger JD, Schaffer AA. PSEUDOMARKER 2.0: efficient computation of likelihoods using NOMAD. *BMC Bioinformatics.* 2014;15:47.

40 Louis ED, Dogu O. Does age of onset in essential tremor have a bimodal distribution? Data from a tertiary referral setting and a population-based study. *Neuroepidemiology.* 2007;29(3-4):208–212.

41 Louis ED, Clark LN, Ottman R. Familial versus sporadic essential tremor: what patterns can one decipher in age of onset? *Neuroepidemiology.* 2015;44(3):166–172.

42 Lander E, Kruglyak L. Genetic dissection of complex traits: guidelines for interpreting and reporting linkage results. *Nat Genet.* 1995;11(3):241–247.

43 Wang GT, Zhang D, Li B, Dai H, Leal SM. Collapsed haplotype pattern method for linkage analysis of next-generation sequence data. *Eur J Hum Genet.* 2015;23(12):1739–1743.

44 Zhao L, He Z, Zhang D, et al. A rare variant nonparametric linkage method for nuclear and extended pedigrees with application to late-onset alzheimer disease via WGS data. *Am J Hum Genet.* 2019;105(4):822–835.

45 Richards S, Aziz N, Bale S, et al. Standards and guidelines for the interpretation of SequenceVariants: a joint consensus recommendation of the American college of medical genetics and genomics and the association for molecular pathology. *Genetics in Medicine.* 2015;17:405–424.

46 Dolzhenko E, Deshpande V, Schlesinger F, et al. ExpansionHunter: a sequence-graph-based tool to analyze variation in short tandem repeat regions. *Bioinformatics.* 2019;35:4754–4756.

47 Stelzer G, Rosen N, Plaschkes I, et al. The GeneCards suite: from gene data mining to disease genome sequence analyses. *Curr Protoc Bioinformatics.* 2016;54:130.1–1.30.33. https://doi.org/10.1002/cpbi.5.

48 Gillespie M, Jassal B, Stephan R, et al. The reactome pathway knowledgebase 2022. *Nucleic Acids Research.* 2021;50:D687–D692.

49 Rai SN, Dilnashin H, Birla H, et al. The role of PI3K/Akt and ERK in neurodegenerative disorders. *Neurotox Res.* 2019;35(3):775–795.

50 Zhou ZD, Sathiyamoorthy S, Tan EK. LINGO-1 and neurodegeneration: pathophysiologic clues for essential tremor. *Tremor Other Hyperkinet Mov (N Y).* 2012;2. https://doi.org/10.7916/D8PZ57JV.

51 Ren X, Aleshin M, Jo WJ, et al. Involvement of N-6 adenine-specific DNA methyltransferase 1 (N6AMT1) in arsenic biomethylation and its role in arsenic-induced toxicity. *Environ Health Perspect.* 2011;119(6):771–777.

52 Tan CX, Eroglu C. Cell adhesion molecules regulating astrocyte-neuron interactions. *Curr Opin Neurobiol*. 2021;69:170–177.

53 Paul S, Dansithong W, Figueroa KP, Gandelman M, Scoles DR, Pulst SM. Staufen1 in human neurodegeneration. *Ann Neurol*. 2021. https://doi.org/10.1002/ana.26515. Online ahead of print.

54 Kiehl TR, Shibata H, Pulst SM. The ortholog of human ataxin-2 is essential for early embryonic patterning in C. elegans. *J Mol Neurosci*. 2000;15(3):231–241.

55 Kiehl TR, Shibata H, Vo T, Huynh DP, Pulst SM. Identification and expression of a mouse ortholog of A2BP1. *Mamm Genome*. 2001;12(8):595–601.

56 Louis ED, Faust PL, Vonsattel JP, et al. Neuropathological changes in essential tremor: 33 cases compared with 21 controls. *Brain*. 2007;130(Pt 12):3297–3307.

57 Louis ED, Babij R, Lee M, Cortes E, Vonsattel JP. Quantification of cerebellar hemispheric purkinje cell linear density: 32 ET cases versus 16 controls. *Mov Disord*. 2013;28(13):1854–1859.

58 Gironell A. The GABA hypothesis in essential tremor: lights and shadows. *Tremor Other Hyperkinet Mov (N Y)*. 2014;4:254.

59 Leveille E, Ross OA, Gan-Or Z. Tau and MAPT genetics in tauopathies and synucleinopathies. *Parkinsonism Relat Disord*. 2021;90:142–154. https://doi.org/10.1016/j.parkreldis.2021.09.008.

60 Cai S, Li J, Wu Y, Jiang Y. De novo mutations of TUBB2A cause infantile-onset epilepsy and developmental delay. *J Hum Genet*. 2020;65(7):601–608.

61 Schmidt L, Wain KE, Hajek C, et al. Expanding the phenotype of TUBB2A-related tubulinopathy: three cases of a novel, heterozygous TUBB2A pathogenic variant p.Gly98Arg. *Mol Syndromol*. 2021;12(1):33–40.

62 Lawson JE, Park SH, Mattison AR, Yan J, Reed LJ. Cloning, expression, and properties of the regulatory subunit of bovine pyruvate dehydrogenase phosphatase. *J Biol Chem*. 1997;272(50):31625–31629.

63 Sorrells S, Carbonneau S, Harrington E, et al. Ccdc94 protects cells from ionizing radiation by inhibiting the expression of p53. *PLoS Genet*. 2012;8(8):e1002822.

64 Romaniello R, Arrigoni F, Fry AE, et al. Tubulin genes and malformations of cortical development. *Eur J Med Genet*. 2018;61 (12):744–754.

65 Ju XC, Hou QQ, Sheng AL, et al. The hominoid-specific gene TBC1D3 promotes generation of basal neural progenitors and induces cortical folding in mice. *Elife*. 2016;5:e18197. https://doi.org/10.7554/eLife.18197.

66 Gengyo-Ando K, Kage-Nakadai E, Yoshina S, et al. Distinct roles of the two VPS33 proteins in the endolysosomal system in Caenorhabditis elegans. *Traffic*. 2016;17(11):1197–1213.

67 Wang JJ, Shan K, Liu BH, et al. Targeting circular RNA-ZRANB1 for therapeutic intervention in retinal neurodegeneration. *Cell Death Dis*. 2018;9(5):540.

68 Liang Z, Liu Z, Cheng C, et al. VPS33B interacts with NESG1 to modulate EGFR/PI3K/AKT/c-Myc/P53/miR-133a-3p signaling and induce 5-fluorouracil sensitivity in nasopharyngeal carcinoma. *Cell Death Dis*. 2019;10(4):305.

69 Polychronopoulos S, Verykokakis M, Yazicioglu MN, Sakarellos-Daitsiotis M, Cobb MH, Mavrothalassitis G. The transcriptional ETS2 repressor factor associates with active and inactive Erks through distinct FXF motifs. *J Biol Chem*. 2006;281(35):25601–25611.

70 Kuo SH, Tang G, Louis ED, et al. Lingo-1 expression is increased in essential tremor cerebellum and is present in the basket cell pinceau. *Acta Neuropathol*. 2013;125(6):879–889.

71 Zia A, Pourbagher-Shahri AM, Farkhondeh T, Samarghandian S. Molecular and cellular pathways contributing to brain aging. *Behav Brain Funct*. 2021;17(1):6.

72 Balali-Mood M, Naseri K, Tahergorabi Z, Khazdair MR, Sadeghi M. Toxic mechanisms of five heavy metals: mercury, lead, chromium, cadmium, and arsenic. *Front Pharmacol*. 2021;12:643972.

73 Eisner A, Pazyra-Murphy MF, Durresi E, et al. The Eya1 phosphatase promotes Shh signaling during hindbrain development and oncogenesis. *Dev Cell*. 2015;33(1):22–35.

74 Merk DJ, Zhou P, Cohen SM, et al. The eya1 phosphatase mediates Shh-Driven symmetric cell division of cerebellar granule cell precursors. *Dev Neurosci*. 2020;42(5-6):170–186.

75 Cook PJ, Ju BG, Telese F, Wang X, Glass CK, Rosenfeld MG. Tyrosine dephosphorylation of H2AX modulates apoptosis and survival decisions. *Nature*. 2009;458(7238):591–596.

76 Krishnan N, Jeong DG, Jung SK, et al. Dephosphorylation of the C-terminal tyrosyl residue of the DNA damage-related histone H2A. X is mediated by the protein phosphatase eyes absent. *J Biol Chem*. 2009;284(24):16066–16070.

77 Ainslie A, Huiting W, Barazzuol L, Bergink S. Genome instability and loss of protein homeostasis: converging paths to neurodegeneration? *Open Biol*. 2021;11(4):200296.

78 Rossi G, Conconi D, Panzeri E, et al. Mutations in MAPT give rise to aneuploidy in animal models of tauopathy. *Neurogenetics*. 2014;15(1):31–40.

79 Vilarino-Guell C, Soto-Ortolaza AI, Rajput A, et al. MAPT H1 haplotype is a risk factor for essential tremor and multiple system atrophy. *Neurology*. 2011;76(7):670–672.

80 Garcia-Martin E, Martinez C, Alonso-Navarro H, et al. H1-MAPT and the risk for familial essential tremor. *PLoS One*. 2012;7(7): e41581.

81 Clark LN, Liu X, Parmalee NL, Hernandez N, Louis ED. The microtubule associated protein tau H1 haplotype and risk of essential tremor. *Eur J Neurol*. 2014;21(7):1044–1048.

82 Farrell K, Cosentino S, Iida MA, et al. Quantitative assessment of pathological tau burden in essential tremor: a postmortem study. *J Neuropathol Exp Neurol*. 2019;78(1):31–37.

83 Pan JJ, Lee M, Honig LS, Vonsattel JP, Faust PL, Louis ED. Alzheimer's-related changes in non-demented essential tremor patients vs. controls: links between tau and tremor? *Parkinsonism Relat Disord*. 2014;20(6):655–658.

84 Kelaini S, Chan C, Cornelius VA, Margariti A. RNA-binding proteins hold key roles in function, dysfunction, and disease. *Biology (Basel)*. 2021;10(5).

85 Jarero-Basulto JJ, Gasca-Martinez Y, Rivera-Cervantes MC, Urena-Guerrero ME, Feria-Velasco AI, Beas-Zarate C. Interactions between epilepsy and plasticity. *Pharmaceuticals (Basel)*. 2018;11(1).

86 Liu-Yesucevitz L, Bassell GJ, Gitler AD, et al. Local RNA translation at the synapse and in disease. *J Neurosci*. 2011;31 (45):16086–16093.

87 Swanger SA, Bassell GJ. Dendritic protein synthesis in the normal and diseased brain. *Neuroscience*. 2013;232:106–127.

88 Hanson KA, Kim SH, Tibbetts RS. RNA-binding proteins in neurodegenerative disease: TDP-43 and beyond. *Wiley Interdiscip Rev RNA*. 2012;3(2):265–285.

89 Gowravaram M, Schwarz J, Khilji SK, Urlaub H, Chakrabarti S. Insights into the assembly and architecture of a Staufen-mediated mRNA decay (SMD)-competent mRNP. *Nat Commun*. 2019;10 (1):5054.

90 Pernice HF, Schieweck R, Jafari M, et al. Altered glutamate receptor ionotropic delta subunit 2 expression in stau2-deficient cerebellar Purkinje cells in the adult brain. *Int J Mol Sci*. 2019;20(7):179. https://doi.org/10.3390/ijms20071797.

91 Zanjani HS, Vogel MW, Mariani J. Deletion of the GluRdelta2 receptor in the hotfoot mouse mutant causes granule cell loss, delayed Purkinje cell death, and reductions in purkinje cell dendritic tree area. *Cerebellum*. 2016;15(6):755–766.

92 Kashiwabuchi N, Ikeda K, Araki K, et al. Impairment of motor coordination, Purkinje cell synapse formation, and cerebellar long-term depression in GluR delta 2 mutant mice. *Cell*. 1995;81 (2):245–252.

93 Pan MK, Li YS, Wong SB, et al. Cerebellar oscillations driven by synaptic pruning deficits of cerebellar climbing fibers contribute to tremor pathophysiology. *Sci Transl Med*. 2020;12(526):eaay1769. https://doi.org/10.1126/scitranslmed.aay1769.

94 Ma F, Dong Z, Berberoglu MA. Expression of RNA-binding protein Rbfox1l demarcates a restricted population of dorsal telencephalic neurons within the adult zebrafish brain. *Gene Expr Patterns*. 2019;31:32–41.

95 Shibata H, Huynh DP, Pulst SM. A novel protein with RNA-binding motifs interacts with ataxin-2. *Hum Mol Genet*. 2000;9 (9):1303–1313.

96 Vollstedt EJ, Kasten M, Klein C, MGGPsDS Group. Using global team science to identify genetic parkinson's disease worldwide. *Ann Neurol*. 2019;86(2):153–157.